PNNL-31934.

# Light Water Reactor Sustainability Program

# Nondestructive Evaluation (NDE) of Cable Moisture Exposure using Frequency Domain Reflectometry (FDR)

September 2021

U.S. Department of Energy

Office of Nuclear Energy

PNNL-31934

## Light Water Reactor Sustainability Program
**Milestone M3LW-21OR0404025**

# Nondestructive Evaluation (NDE) of Cable Moisture Exposure using Frequency Domain Reflectometry (FDR)

**S.W. Glass, M.P. Spencer, A. Sriraman, L.S. Fifield, M. Prowant**

**Pacific Northwest National Laboratory**

**September 2021**

**Prepared for the**
**U.S. Department of Energy**
**Office of Nuclear Energy**

# SUMMARY

This Pacific Northwest National Laboratory (PNNL) milestone report assesses the capability of frequency domain reflectometry (FDR) to determine electrical cable submergence using PNNL's Accelerated and Real-Time Environmental Nodal Assessment (ARENA) cable/motor test bed. This work includes a review of relevant literature as well as experimental tests.

Nuclear power facilities have experienced various electrical cable failures related to water exposure. The current industry response involves actions to de-water cable vaults, manholes, and other cable locations. These efforts require considerable expenditure of resources, which makes it desirable for the industry to have information on cable condition and history regarding their submergence and water exposure (Mantey 2012).

Two tests that are gaining favor within the nuclear industry are time-domain reflectometry (TDR) and FDR. These are low-voltage nondestructive tests that can be applied at a cable end. Testing from the cable end is important because local inspection along the cable length is very difficult due to cables being routed within trays, conduits, underground, and through walls. Both TDR and FDR techniques have been shown to locate cable insulation damage due to thermal, radiation, and mechanical damage. FDR measurements are also more sensitive than TDR to temperature changes, small-bend radius bends, and cable contact with various materials, including conductive materials like steel and water. This work evaluates the feasibility to extend FDR testing to characterize whether an electrical cable is submerged or not and where it may be submerged using PNNL's ARENA cable/motor test bed.

Shielded and unshielded cables were evaluated using FDR conductor-to-conductor for unshielded and conductor-to-shield for shielded cables. Observations and conclusions are as follows:

- FDR shows the presence/absence of water with non-shielded cable.
- No peaks were observed indicating presence/absence of water with shielded cable.
- FDRs were equivalent with and without a motor being connected.
- Water detection was frequency dependent – 100MHz was clearer than 1.3GHz.
- ARENA test bed enabled quick evaluation.

# ACKNOWLEDGMENTS

This work was sponsored by the U.S. Department of Energy, Office of Nuclear Energy, for the Light Water Reactor Sustainability (LWRS) Program Materials Research Pathway. The authors extend their appreciation to Pathway Lead Dr. Thomas Rosseel for LWRS programmatic support. This work was performed at the Pacific Northwest National Laboratory (PNNL). PNNL is operated by Battelle for the U.S. Department of Energy under contract DE-AC05-76RL01830.

# CONTENTS

# FIGURES

# TABLES

# ACRONYMS AND ABREVIATIONS

| | |
|---|---|
| AMP | Aging Management Program |
| AMS | Analysis and Measurement Services |
| ARENA | Accelerated and Real-Time Environmental Nodal Assessment |
| ASIC | application-specific integrated circuit |
| c | speed of light or 299,792,458 m/s |
| C | Capacitance (for cable, expressed as pF or pico-Farads/inch) |
| CPE | chlorinated polyethylene |
| DBE | design-basis event |
| Dk | dielectric constant |
| EPR | ethylene propylene rubber |
| EPRI | Electric Power Research Institute |
| $\varepsilon_\Upsilon$ | dimensionless relative insulation permittivity |
| $\rho$ | FDR reflection coefficient = Reflected/Incident |
| FDR | frequency domain reflectometry |
| FFT | fast Fourier transform |
| HV | high-voltage |
| I | Current (for RF current, expressed as complex number) |
| L | Inductance: for cable expressed as nano(n)-Henries/inch |
| LIRA | line resonance analysis |
| LOCA | loss-of-coolant accident |
| LV | low voltage |
| LWRS | Light Water Reactor Sustainability Program |
| MCR | multicarrier reflectometry |
| MSR | mixed signal reflectometry |
| NDE | nondestructive evaluation |
| NPP | nuclear power plant |
| NRC | U.S. Nuclear Regulatory Commission |
| PNNL | Pacific Northwest National Laboratory |
| PVC | polyvinyl chloride |
| RF | radio frequency |
| SLR | subsequent license renewal |
| SSTDR | spread spectrum time domain reflectometry |
| S/SSTDR | sequence/spread spectrum time domain reflectometry |

| | |
|---|---|
| SWR | standing wave reflectometry |
| TDR | time domain reflectometry |
| TEM | transverse electromagnetic |
| V | Voltage (for RF voltage, expressed as complex number) |
| $V_{incident}$ | Incident Velocity |
| $V_{reflected}$ | Reflected Velocity |
| VNA | vector network analyzer |
| XLPE | cross-linked polyethylene |
| $X_L$ | Inductive part of complex Impedance |
| $X_C$ | Capacitive part of complex impedance |
| Z | complex impedance |
| $Z_0$ | Real part of complex impedance (ohms) |

# 1. OBJECTIVES

This Pacific Northwest National Laboratory (PNNL) milestone report describes the investigation of nondestructive test methods to extend frequency domain reflectometry (FDR) measurements beyond traditional applications and focus on moisture and submergence detection of electrical cables. This work includes:

a. A review of FDR theory and relevant publications related to cable moisture detection.

b. A description of the Accelerated and Real-Time Environmental Nodal Assessment (ARENA) cable/motor test bed and how this was used for FDR moisture detection.

c. Moisture/water detection results.

d. Observations and conclusions.

This report is submitted in fulfillment of deliverable M3LW-210R04025-NDE tests of cable motor systems with and without coupling and decoupling motor connections.

This work is part of an overall project to develop technical basis for assessing the level and impact of cable insulation aging and degradation in nuclear power plants (NPPs). PNNL has developed capabilities for thermal, radiation, and combine thermal and radiation aging of cables as well as significant capability to test and evaluate cable conditions (Fifield et al. 2015, Glass et al. 2015, Glass, Fifield, and Hartman 2016, Glass et al. 2017, Glass et al. 2018, Glass S.W. 2020). In July 2012, a workshop was held at PNNL to lay the groundwork for a research and development roadmap to address aging cable management in NPPs particularly focused on nondestructive examination (Simmons et al. 2012). This work is a direct extension of that plan.

# 2. INTRODUCTION AND BACKGROUND

Currently, many nuclear power plants (NPPs) are considering applying for a second, or subsequent, license renewal (SLR) to extend their operating period from 60 years to 80 years (NRC 2021). For SLRs it is important to understand how materials installed in plant systems and components will age during that time and to develop aging management programs to assure continued safe operation under normal and design-basis events (DBE). As such, most NPPs now have cable management programs that involve nondestructive evaluation (NDE) to assure electrical cable performance. However, utilities are constantly looking for additional and improved ways to use their NDE information or online monitoring techniques to better inform plant decisions.

Some electrical equipment (including cables) exposed to water may experience aging (Tomain G. 2004)Reductions in the integrity of electrical equipment due to moisture can affect the ability of equipment to perform its intended function. Damage to electrical equipment can also result from flood waters contaminated with chemicals, sewage, oil, and other debris, which will affect the integrity and performance of the equipment. It is desirable to extend existing cable evaluation techniques, particularly online monitoring, to characterize whether a cable is submerged in water or not and to locate where it may be submerged.

One test that has attracted significant attention in recent years is frequency domain reflectometry (FDR). This is a low-voltage nondestructive test that can be applied at a cable end. Testing from the cable end is important because local inspection along the cable length is very difficult due to cables being routed within trays, conduits, underground, and through walls thereby limiting physical access. FDR has been shown to locate electrical cable insulation damage due to thermal, radiation, and mechanical damage. PNNL has evaluated several types of FDR test equipment to produce the general observations shown in Table 2.1 (Glass et al. 2016a).

While current commercial offerings do not allow FDR coupling to live power cables, this work is focused on the feasibility of FDR to detect the presence or absence of water. Time domain reflectometry (TDR) systems can be coupled to live power systems and TDR coupling filters can likely be adapted to FDR technology, but TDR is not as sensitive to insulation degradation and the surrounding environment as FDR and therefore is not the focus of this work.

Table 2.1. Advantages and Disadvantages of FDR Testing

| | |
|---|---|
| Advantages | • Inspection of entire cable length from single-ended access<br>• Low voltage, nondestructive test<br>• Rapid inspection times (several minutes)<br>• Systems commercially available<br>• Sensitive detection and location of localized degradations<br>• In most cases, there is no need to de-terminate one or both cable ends |
| Disadvantages | • Global aging indicators still in development for correlation to established methods<br>• Baseline data sets helpful to assess cable condition<br>• Specialized training required for system operation and data analysis<br>• Cannot currently be used on energized cables like SSTDR but should be possible with similar isolation circuits |

# 3. TIME DOMAIN (TDR) AND SPREAD SPECTRUM (SSTDR) REFLECTOMETRY

Prior to discussing FDR, it is helpful to understand TDR, particularly as there are numerous examples of TDR detecting water or cable submergence. TDR measures reflections of a stepped or impulse signal along a single conductor to detect and locate any changes in the conductor or insulation impedance (Glass et al. 2015). A TDR pulse is usually less than 10 volts and is primarily in the higher frequency range (> 1 kHz), so the pulse has little or no effect on low frequency signals or on 50/60 Hz power excitation. TDR transmits an incident signal into the conductor and listens for signal reflections. If the conductor is a uniform impedance network and is terminated to a matching impedance, then there will be no reflections and the transmitted signal will be completely absorbed at the far end by the termination. Instead, if there are impedance variations as in a short or open circuit at the cable end, a damaged or reduced cross-sectional area, or a splice with a higher resistance along the conductor, then some fraction of the incident signal will be reflected to the source. The polarity of the reflection contains information about the reflector. An open cable end will reflect "in-phase" with the excitation and a short will reflect as an inverted signal. This reflected signal is measured at a point in time on the TDR instrument that is proportional to the signal propagation velocity in the cable and the distance along the cable, thereby allowing assessment of the location of any reflector observed. The amplitude of the reflected signal coupled with the inherent cable attenuation characteristics also allows an estimate of the magnitude of the impedance change. An example TDR test setup and plot is shown in Figure 3-1 (IAEA 2012).

TDR testers are portable units that can easily be used in-situ within an NPP. The test is a low-voltage (LV) test so there is virtually no risk to the cable. The main emphasis, however, of a portable TDR tester is to assess cable condition, faults, or anomalies in the conductor. Very little information is provided regarding subtle changes in the insulation as would be anticipated from early stages of cable aging insulation degradation. Moreover, these units are not intended to be operated on live wires and in fact most have a warning indication if a voltage is detected on the test wire (Megger 2020).

Several enhancements to the traditional TDR measurement are available today for locating electrical faults based on reflectometry concepts. These include standing wave reflectometry (SWR), mixed signal reflectometry (MSR) (Tsai et al. 2005), multicarrier reflectometry (MCR) (Naik, Furse, and Boroujeny 2006) and sequence/spread spectrum time domain reflectometry (S/SSTDR) (Smith, Furse, and Kuhn 2008). For online applications, S/SSTDR has been most fully exploited in the aircraft industry and the rail industry where low-cost ASIC-based instruments have been developed for online monitoring of control and power circuits up to 1000 volts.

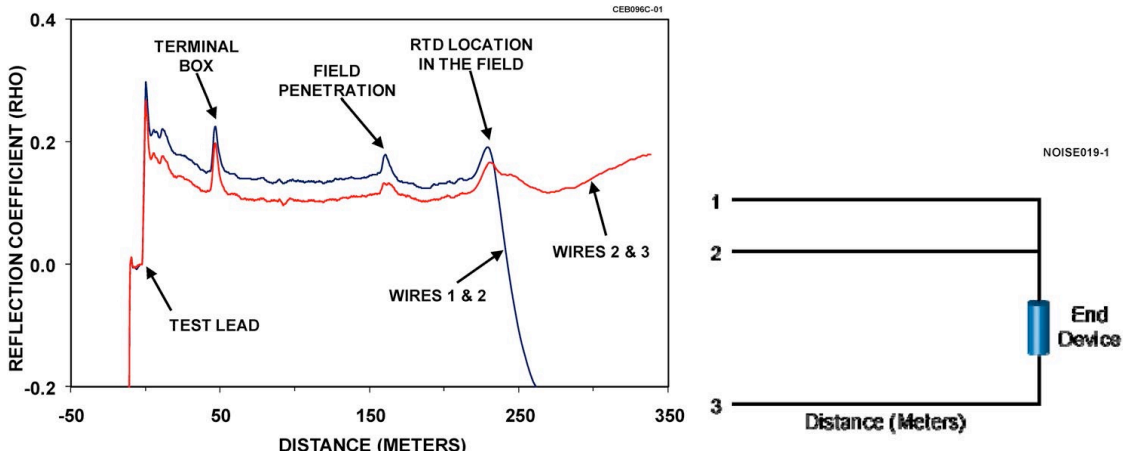


Figure 3-1. Typical test plot of a 3-conductor TDR (left) and a schematic of the corresponding TDR test setup (right) (IAEA 2012).

# 4. FREQUENCY DOMAIN REFLECTOMETRY (FDR)

FDR is a nondestructive electrical inspection technique used to detect, localize, and characterize subtle impedance changes in power and communication system conductors and insulation materials along the length of a cable from a single connection point. FDR is based on the interaction of electromagnetic waves with conductors and dielectric materials as they propagate along the cable. The technique uses the principles of transmission line theory to locate and quantify impedance changes in the cable circuit. These impedance changes can result from connections, faults in the conductors, or degradation in the cable polymer material (Furse, Chung, Dangol, et al. 2003, Agilent 2012). In this section, FDR theory is first addressed generally and then implementation of this theory is addressed specifically for typical instruments used to measure the FDR response.

For an FDR measurement, two conductors in the cable system are treated as a transmission line through which a low-voltage swept-frequency waveform is propagated. As the excitation signal is swept over the frequency range and the associated electromagnetic wave travels down the cable, the impedance response is recorded at each frequency to characterize wave interaction with the conductors and surrounding dielectric materials. The remote end of the cable can be terminated in an arbitrary impedance different from the cable characteristic impedance but is often grounded or open-circuited during testing. Because the applied signal is low-voltage, the test is nondestructive and poses no special safety concerns to operators assuming that routine electrical safety procedures are followed (Glass et al. 2017). In most cases, it is only necessary to de-energize the cables and de-termination is not required, but typically at least one end of the cabling is de-terminated to connect the FDR system. Only de-terminating one cable end can be an advantage over many other techniques by shortening the required testing time and minimizing the risk of improper re-termination. Frequently, however, both ends of the cable systems are de-terminated anyway to minimize the risk of residual charge shock and in some cases, reduce noise on the FDR signal.

A linearly increasing “chirp” sinusoidal waveform is shown in Figure 4-1 that is representative of the type of excitation signal used in the FDR technique. The excitation signal can be generated for transmission into the cable using an analog circuit, such as a voltage-controlled oscillator or using a digital circuit such as a direct digital synthesizer.

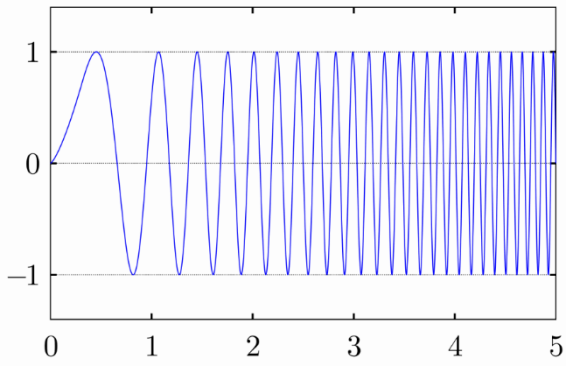


Figure 4-1. Example FDR “chirp” excitation waveform in which the signal frequency linearly increases as a function of time.

A representation of the electric and magnetic vector field components for a propagating sinusoidal transverse electromagnetic (TEM) wave is shown in Figure 4-2 (a). For TEM waves traveling on a transmission line, the electric and magnetic fields are orthogonal to each other as well as the direction of propagation. In Figure 4-2 (b), cross-sectional views of the electric and magnetic field configurations for TEM waves traveling on coaxial and two-wire transmission lines are shown. The electric field starts and ends on current-carrying conductors and are influenced by dielectric materials and other metals. The magnetic field forms closed loops around the current-carrying conductors and are influenced by magnetic materials.

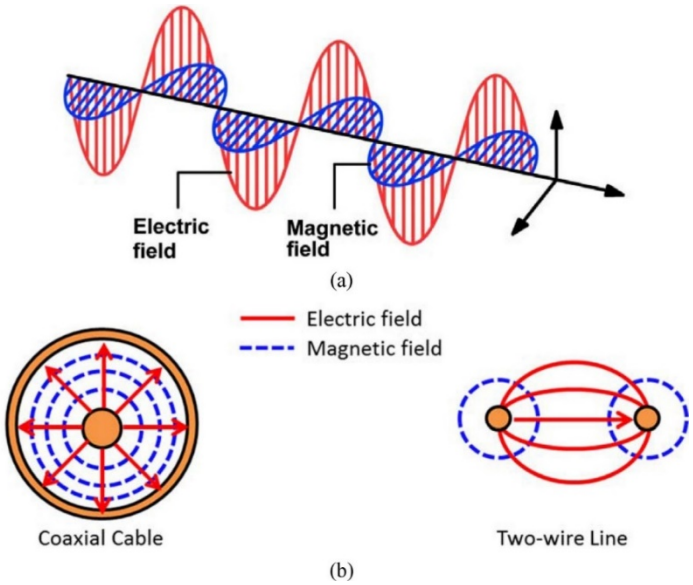


Figure 4-2. (a) Electric and magnetic field configurations for generalized sinusoidal TEM wave propagation. (b) Electric and magnetic field configurations for specific cable types (Glass et al. 2017)

While TEM wave propagation analysis may be complicated by unknown and changing electromagnetic properties of the waveguide, for most practical applications a simplified form of analysis referred to as transmission line theory is sufficient (Glass et al. 2017). In transmission line theory, the electric field is related to the distributed (per unit length) capacitance and the magnetic field is related to the distributed inductance. The resistance of the metallic conductors and dielectric loss in the insulation attenuate the signal as it propagates along the cable. A schematic representation of the standard transmission line model is shown in Figure 4-3, where the distributed circuit elements representing an infinitesimally short length may be cascaded with similar elements to model the overall behavior of the line. In the FDR method, an inverse Fourier transform coupled with the cable velocity factor is used to obtain the range domain data, which contains information on the wave interactions with the cable's resistive, inductive, and capacitive material and which identifies the physical location of signal reflections (Minet et al. 2010).

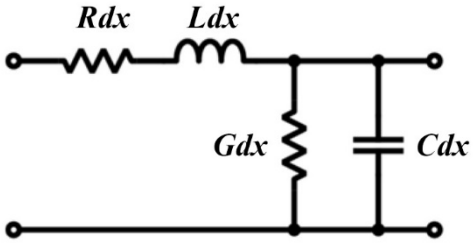


Figure 4-3. Transmission line RLGC circuit model consisting of distributed impedance elements over an infinitesimally short length.

The FDR technique can potentially yield better sensitivity to cable degradations than traditional time domain reflectometry (TDR), which is better suited for identifying open and short circuit conditions in the conductors (Murty 2013). For example, FDR is less susceptible to electrical noise and interference due to the availability of filtering and noise-lowering algorithms in the frequency domain (IEC 2002). This can lead to increased sensitivity and accuracy. In addition, TDR pulses may have difficulty continuing in the forward direction after several significant reflections or multiple reflections. This may complicate the correlation between the impedance change and the corresponding location on the reflectometry waveform. Conversely, FDR has a high dynamic range and is better suited for identifying and characterizing a series of multiple degradations in long cables.

The spatial resolution is an important parameter for detection and localization of cable defects. The resolution is a function of the swept-frequency bandwidth (BW), the speed of light (c), and the velocity factor (VF) of the cable (Mohr and Associates 2010):

$$\text{Resolution (m)} = (c \times VF) / (2 \times BW) = 1.5\text{E}8 \times (VF/BW) \quad (4.1)$$

where $c = 3 \times 10^8$ m/s. The cable's *VF* is a value less than unity and is inversely related to the square root of the dielectric constant of the insulation material. As an example, using a 200 MHz FDR bandwidth to inspect a coaxial cable with a velocity factor of 66% results in a 0.5 m resolution as shown below:

$$\text{Resolution} = 3\text{E}8\text{m} * 0.66/ (2*2\text{E}8) = 0.5 \text{ m} = 1.6 \text{ ft} \quad (4.2)$$

The maximum unambiguous (alias-free) range is also a factor for interpreting FDR results and is a function of the resolution and the number of frequencies (*NF*) used to cover the bandwidth (Mohr and Associates 2010):

$$\text{Range (m)} = \text{Resolution} \times NF \quad (4.3)$$

Another important parameter in the implementation of the FDR method is the bandwidth of the swept-frequency signal that propagates along the cable. A higher bandwidth waveform allows for increased detection sensitivity, a shorter termination shadow, and improved localization of degradations due to better spatial resolution. However, higher bandwidth signals are more susceptible to signal attenuation along the cable, which can limit the inspection length. If the maximum frequency is too low, the cable length will not be sufficient to be treated as a transmission line and the measurement may not produce meaningful results. Typically, the electrical length of the cable should be at least one wavelength of the signal propagating along the cable to apply radio-frequency transmission line theory. Thus, higher frequencies are required to characterize shorter cables to satisfy the cable length requirement and lower frequencies are required to characterize longer cables to prevent the insertion loss from overcoming the measurement signal.

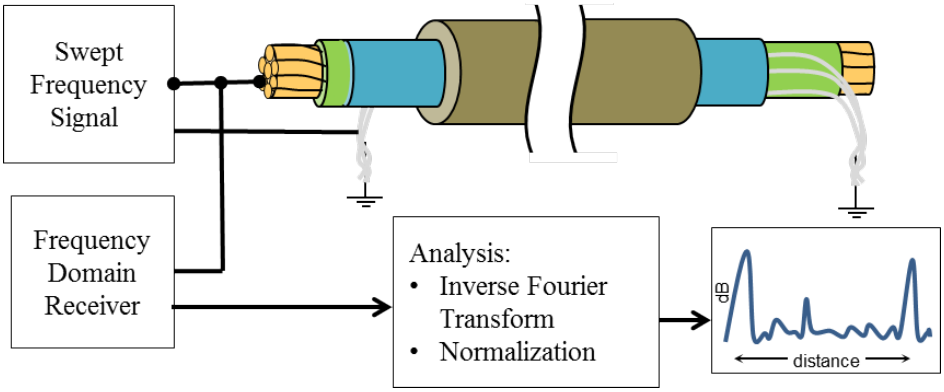


Figure 4-4. Block diagram of FDR instrument and cable test arrangement.

Figure 4-4 shows a simplified diagram and example data processing flow for an FDR system, which collects and processes cable data for aging or damage evaluation. The signal reflections measured by the FDR system are caused by changes in the characteristic impedance (*Z*) along the length of cable. Physical changes such as cuts, gouges, and excessive bending or thermal and radiation aging-related degradation of the cable insulation are among causes for *Z* changes. As an example, the characteristic impedance of the twisted-pair cable shown in Figure 4-5 can be calculated using the following equation (EE_Web 2015, Apogeeweb_Semiconductor_Electronic 2016)

$$Z = V/I = Z_o + j*(X_L - X_C) \quad (4.4)$$

$$Z_0(ohms) = \frac{120}{\sqrt{\varepsilon_r(f)}} \times ln(\frac{2S}{D}) \quad (4.5)$$

$$X_L = \omega L \tag{4.6}$$

$$Xc = 1/\omega\, C \tag{4.7}$$

$$Z = Z_0 + j*(X_L - X_C) \tag{4.8}$$

$$C\ (pF/inch) = \frac{0.7065}{Ln(2S/D)} \times \varepsilon_Y \tag{4.9}*$$

$$L\ (nH/inch) = 10.16 * 10^{-9} * \ln(2*S/D) \tag{4.10}$$

where Z is the Cartesian coordinate complex expression of impedance, $Z_0$ is the real impedance component (ohms), $X_L$ is the inductive impedance component, $X_C$ is the capacitive impedance component *S* is the distance between the two conductors (as *S* and *D* are expressed as a length ratio, units are unimportant as long as they are the same units), *D* is the conductor diameter, *f* is the frequency, $\omega = 2*\pi*f$, and $\varepsilon_r$ is the dimensionless relative permittivity of the insulation material.

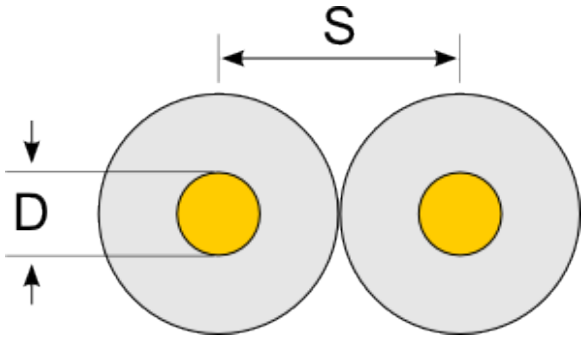


Figure 4-5. Cross-sectional view of commonly used twisted-pair cable.

Based on the above equation, parameters that could create a change in the characteristic impedance are the physical dimensions and the relative permittivity of the insulation material. Physical damage to the jacket material or excessive bending would cause changes in the spacing of the cable conductors. Because there is no significant change in the spacing or diameter of the conductors during the aging process, the relative permittivity is the only remaining variable that could change the impedance and cause reflections in FDR data The relative permittivity is directly related to the capacitance of the cable using the insulation material as the dielectric media:

Capacitance changes from insulation aging can be monitored over time using FDR measurement. The reflections of the FDR signal are converted from frequency to the time domain using an inverse fast Fourier transform. In the time domain, the impulse response data is further enhanced by integrating over time to obtain the step response. The result of the integral is expressed in terms of the reflection coefficient ($\rho$) as:

$$\rho = \frac{V_{reflected}}{V_{incident}}. \tag{4.11}$$

The distance to fault is calculated using the velocity factor for the cable, which is a percentage of the speed of light in a vacuum and is determined by the relative permittivity of the cable's insulating material. Distance to fault can be determined by multiplying the signal propagation velocity of the cable ($V_P = c$ x *VF*) by half the time (T) it takes for the incident wave to travel to the impedance change and be reflected back to the signal generator . Most of the subsequent FDR responses are shown as time/distance responses where distance is related to time by equation 4.12.

$$\text{Distance} = \frac{V_P T}{2}. \tag{4.12}$$

In general, FDR data can be viewed in two forms – the impulse response and the step response – depending on the desired analysis to be performed. The impulse response, $h(t)$, is shown in Equation 4.13 through the inverse Fourier transform of the transfer function, where $H(f)$ is the FDR return loss as a function of frequency.

$$h(t) = \int_{-\infty}^{\infty} H(f) e^{j2\pi ft} df \tag{4.13}$$

The step response, $f_{step}(t)$, is given by integration of the impulse response as shown in Equation 4.14

$$f_{step}(t) = \int_{-\infty}^{\infty} h(t) dt \tag{4.14}$$

Examples of FDR impulse and step time/distance response are shown in Figure 4-6 through Figure 4-8. Figure 4-6 and Figure 4-7 are sample data provided over two different frequency bandwidths for the same measured cable response. Figure 4-8 shows the impulse and step response for a mechanically damaged cable with the mechanical insulation damage at approximately 50-ft or near the cable mid-point.

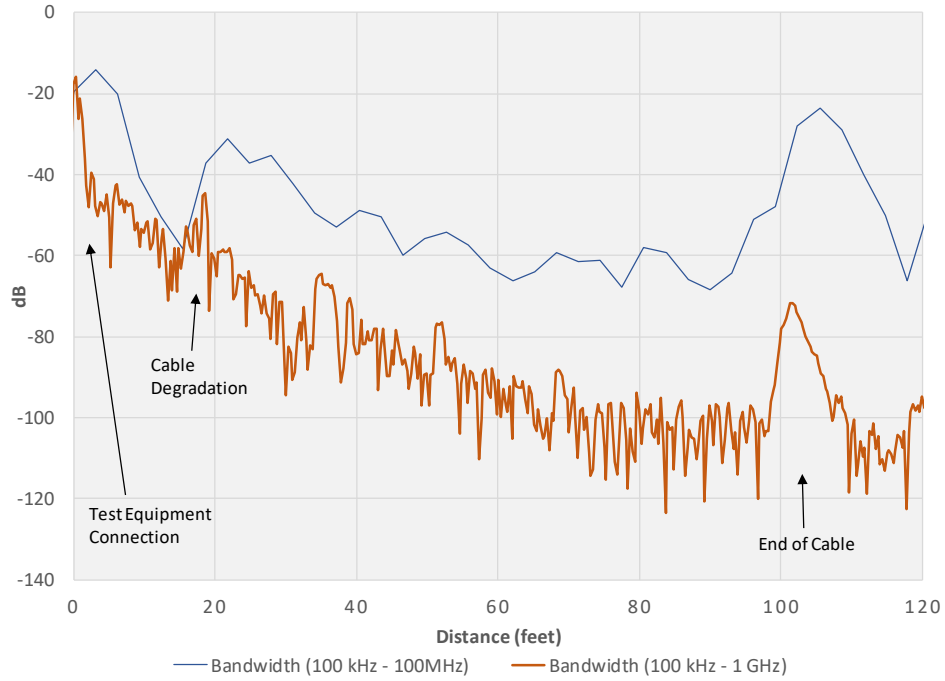


Figure 4-6. Example FDR impulse response data. Figure courtesy of AMS Corporation (Glass et al. 2016b).

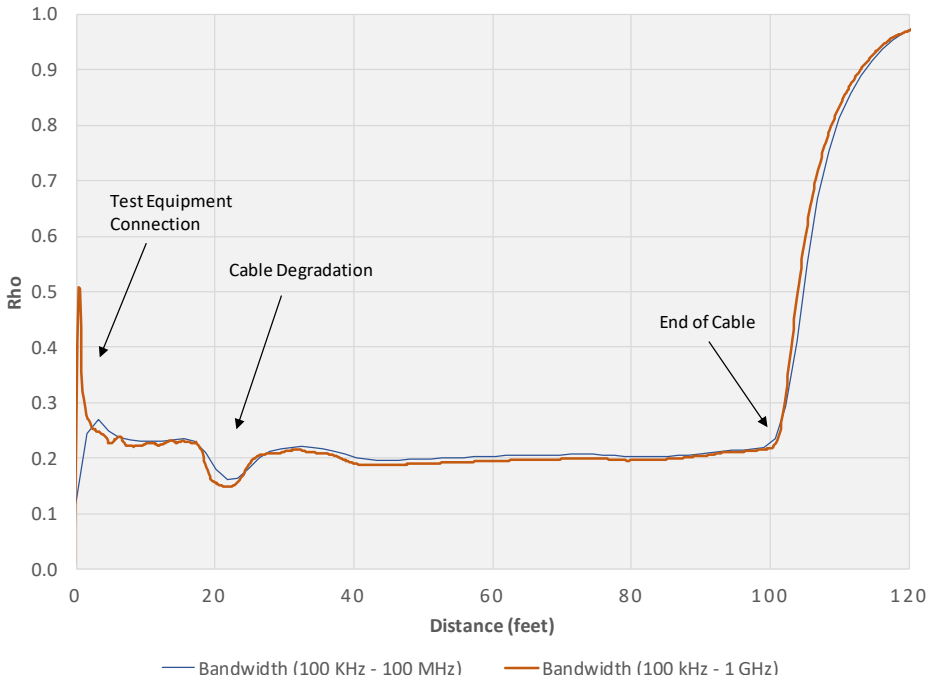


Figure 4-7. Example FDR step response data. Figure courtesy of AMS Corporation [(Glass et al. 2016b)].

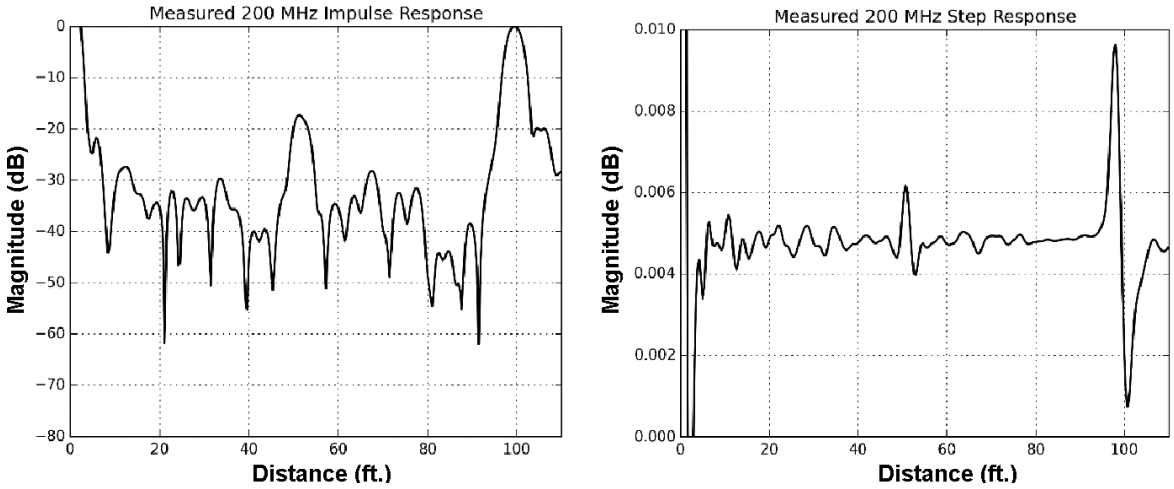


Figure 4-8. Measured FDR response for a shielded triad cable with mechanically damaged defect at mid-point: (*left*) impulse response and (*right*) step response [(Glass et al. 2016b)].

# 5. COMPARISON OF TDR AND FDR

FDR and TDR analyzers are generally sensitive to cable impedance changes. However, in practice, they are more or less sensitive to different characteristics (IWCE 1996). TDR is sensitive to lumped-dc parametric characteristics but is likely to miss RF characteristics such as corrosion, slight pin gaps, and damaged RF components. TDR also has severe difficulty "seeing" past any RF component with a passband characteristic, such as filters, duplexers, quarter wave lightning arrestors, and antennas. Another basic limitation of TDR techniques is tied to frequency-selective performance issues. These issues are caused by a large proportion of DC spectral content of the TDR's stimulus signal. The FDR technique is more highly sensitive to any dimensional tolerance change within the RF conductor path including even small variation in return loss, such as connector corrosion or a weak contact.

A study performed in 2006 (Furse et al. 2006) compared several types of reflectometry systems focusing on aircraft wiring networks. The systems reviewed are summarized below in Table 5-1.

Table 5-1. Comparison of reflectometry methods

| Wire Fault Sensor | Accuracy (in) | Min Length (in) | Estimated Max Length (ft) | Computation | Network Topology Recognition |
|---|---|---|---|---|---|
| TDR (Megger 2020) | 6-12 | 5 | 100+ | Edge Identification | Yes |
| FDR (Furse, Chung, Rakesh, et al. 2003) (Furse et al. 2005) | 2 | 4 *** | 50+ | FFT; Peak Identification | Yes |
| S/SSTDR (Furse et al. 2005); (Smith 2003) | 1 | 4 | 70+ | Peak Identification | Yes |
| Capacitance or Capacitance/Inductance Sensor (Chung, Amarnath, and Furse 2009) | 1 | 1 | 100+ | Linear Curve Fit | No |

This report focuses on FDR performance because it is believed to be more sensitive to water detection, although there are examples where readily implementable TDR techniques have also successfully located water (discussed in the next section).

# 6. MOISTURE DETECTION

In this section, a brief overview of moisture detection by FDR and TDR techniques is discussed. Modeling data for unshielded 3-conductor cable was shown to predict a slight (3-dB) FDR sensitivity to the presence or absence of water (Glass et al. 2017). This study also noted that the amplitude response of an FDR signal was dependent on the profile of the damaged or exposed portion of the cable and would be strongest for a 2-3ft. segment. For longer segments, the response morphed to 2 peaks corresponding to the beginning and end of the damaged or exposed portion of the cable.

Stepped frequency chirp TDR measurements have been applied (Giaquinto N. 2019) to locate leaks in piping systems. There was no distinction to separate the pipe fault from moisture in this work, but evidence was clear that leaks could be identified and located with a modified TDR technique.

Time-domain reflectometry has been cited as a well understood and possible measurement method to measure liquid level within a nuclear reactor (Anderson 1980). A simple probe is envisioned as a long rod, possibly shielded from contacting the internal components of the reactor. The electronic hardware is available off the shelf as oscilloscope plug-in modules. This self-calibrating and self-verifying system compares the delay times of pulses reflected from the end of the sensor with the delays resulting from reflections caused by the change in impedance at the vapor-water interface. A serious disadvantage is that any contact along the length of the sensor would also generate a reflection.

In order for an FDR or TDR system to monitor live cable systems, an electrical coupler must be attached to the cable system. (Dubickas V. 2004) reviewed capacitive and inductive coupling approaches to couple TDR high frequency signals to 50/60Hz power cable systems. They concluded that it is possible to inject the signal used for TDR diagnostics through the coupler to the power cable and detect its reflections by the same coupler during on voltage power cable operation. Both inductive and capacitive couplers were investigated. Advantages of the capacitive coupling were lower noise and better high frequency signal fidelity, while a disadvantage included the requirement to connect directly to a conductor. Inductive coupling brings the advantage that the transformer is wrapped around the outside of the insulation without direct contact to the conductor. This type of coupling will be easier to implement in a power plant

environment because the sensor only touches the outside of the insulation – not the conductor. The drawback, however, is that the high frequency signal fidelity is poorer for induction coupling. The capacitive coupler's width and position on a single-phase HV termination must be carefully selected to avoid corona discharges. SSTDR couplings are available with both kinds of couplers however, no commercially available FDR systems are currently available for live wire connections.

# 7. ARENA CABLE/MOTOR TEST BED

For evaluation of FDR for moisture detection, PNNL's ARENA cable/motor test bed was used. This facility includes a 480VAC 3-phase motor that can be connected to a power supply. Cables may be routed through an oven for thermal stressing and through a water bath. The test facility schematic is shown in Figure 7-1.

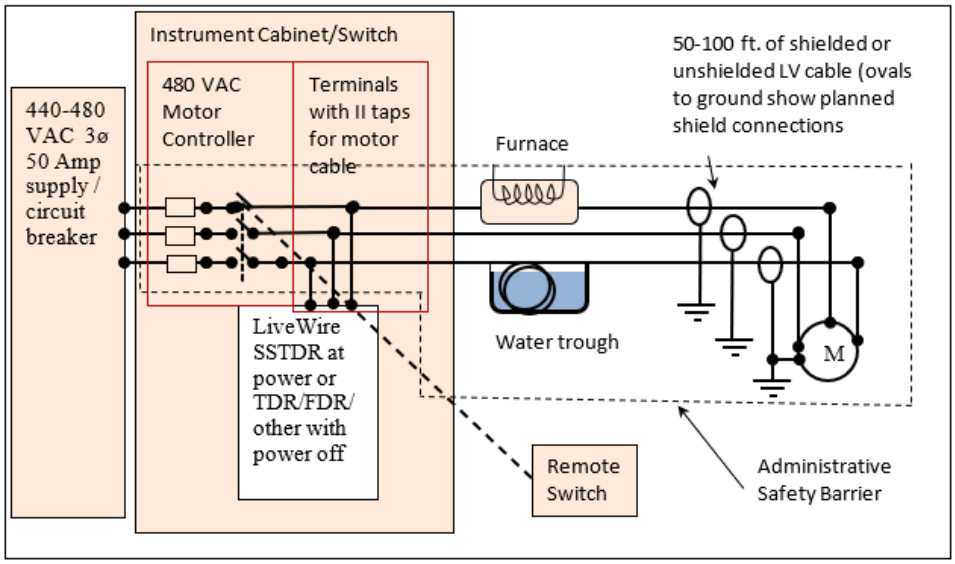


Figure 7-1 Schematic of the ARENA cable/motor test bed at PNNL

# 8. TEST SETUP

The cables selected for evaluation are shown in Table 8-1. The cables had three 14 AWG conductors with a voltage rating of 600 V, EPR insulation, and CPE jacket. For reflectometry measurements, the cables were not energized (i.e., they were disconnected from a power source). To facilitate FDR measurement, a compact VNA (Copper_Mountain 2020) was connected at one end of the cables as shown in Figure 8-1. Details regarding settings of the VNA at each evaluated bandwidth are shown in Table 8-2. The velocity factor was selected as 0.66 for all measurements and the number samples in the frequency domain was chosen to be 1024 to ensure propagation of the signal down the entirety of the cable at all bandwidths.

Table 8-1. Manufacturer information for the cables selected for evaluation.

| Manufacturer | P/N | Jacket | Insulation | Type |
|---|---|---|---|---|
| General Cable | 354800 | CPE | EPR | Shielded |
| | 6-903-SH 14AWG-3/C FR-EP 600V FR-EPR/CPE Foil Shielded 600V E-2 | | | |
| General Cable | 383830 | CPE | EPR | Non-Shielded |
| | 6-903-G 14AWG-3/C FR-EP 600V FR-EPR/CPE Non-Shld 600V E-2 | | | |

Table 8-2. VNA settings for FDR measurement.

| Bandwidth | Spatial Resolution (ft) | Range or Propagated Length of Signal (ft) | Number of Samples (#) | Velocity Factor |
|---|---|---|---|---|
| 300 kHz to 100 MHz | 3.3 | 3330 | 1024 | 0.66 |
| 300 kHz to 500 MHz | 0.6 | 664 | 1024 | 0.66 |
| 300 kHz to 1.30 GHz | 0.2 | 225 | 1024 | 0.66 |

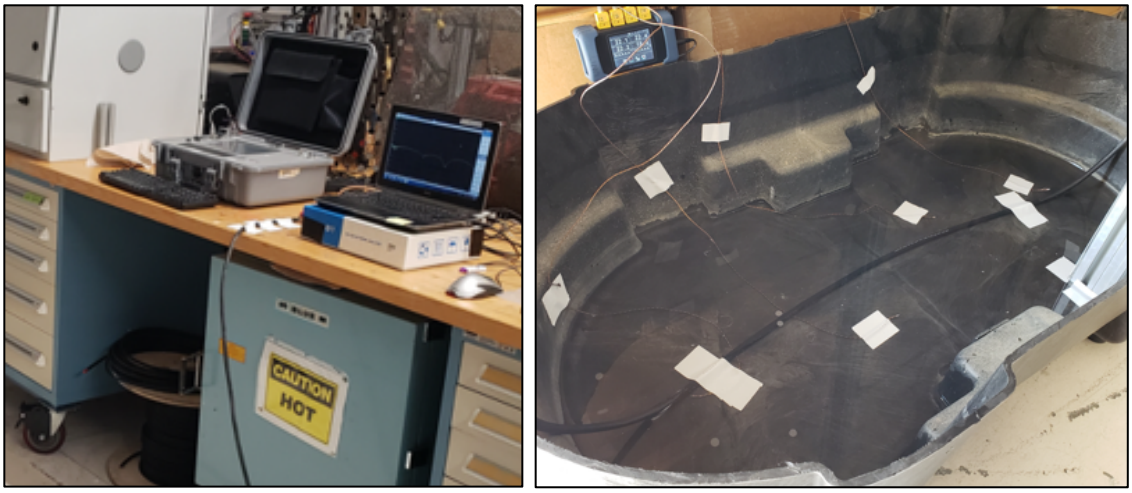


Figure 8-1. Experimental setup for moisture detection using FDR: VNA and computer to left; water bath with cable to right.

Prior to attachment to the VNA, the cables were gently unrolled from a spool to a length of approximately 90 ft (91.4 ft ± 1 ft for the shielded cable and 87.1 ft ± 1 ft for the non-shielded cable) with care being taken to ensure no artificially imposed impedance variations due to bending of the cable. At approximately 60 ft (59.4 ft ± 1 ft for the shielded cable and 54.7 ft ± 1 ft for the non-shielded cable) the cables were routed through a 3 ft long water bath. The water bath depth was measured as 0.28 in and FDR measurements were conducted on the cables with and without the water present (the cables were not moved between measurements). Details regarding location of expected impedance discontinuities are shown in Table 8-3. During attachment of the cables to the VNA, care was taken to reduce impedance mismatch at 0 ft. For the shielded cable, the shield was selected as one of the conductors as it was hypothesized that the effect of water would be more pronounced in this test configuration. For connection to the motor, the conductors that would be energized if the motor were running were attached to the white and orange leads.

Each FDR measurement was conducted at ambient conditions (22°C, 30% relative humidity). The FDR measurement process for each cable (shielded and non-shielded) was as follows: 1) no water present and the cables were open-ended, 2) no water present, but the cables were attached to the motor, 3) water present and the cables were attached to the motor, and 4) water present and the cables were open-ended. At each condition, one measurement per frequency bandwidth was collected.

Processing of the collected FDR results was done in Matlab. The frequency domain information was converted into time domain using inverse Fourier transform without zero padding.

Table 8-3. Measured locations of expected impedance variations.

| Cable Type | Location of Cable Impedance Changes | | | | | |
|---|---|---|---|---|---|---|
| | VNA | Termination | Enter Bath | Exit Bath | Termination | Open/Motor |
| Shielded | 0 ft | 1.6 ft | 59.4 ft | 64.0 ft | 90.4 ft | 91.4 ft |
| Non-Shielded | 0 ft | 1.6 ft | 54.7 ft | 59.3 ft | 86.6 ft | 87.1 ft |

# 9. RESULTS

In FDR analysis, the spatial resolution and bandwidth of the swept-frequency signal that propagates the length of the cable are two important parameters to consider when determining the location of a cable defect. For this study, the bandwidths and the corresponding spatial resolutions are shown in Table 8-2. The magnitude (in dB) of the measured frequency domain response of the shielded and unshielded cables (no water present and not connected to the motor) at the three chosen bandwidths are shown in Figure 9-1. Although a higher bandwidth (1.3 GHz) provided an increased spatial sensitivity to impedance variations, these signals are also more susceptible to attenuation when propagating along the cable length. On the other hand, while spatial resolution decreases at lower bandwidths (e.g., 100 MHz), signal strength improves enabling interrogation of longer cable lengths.

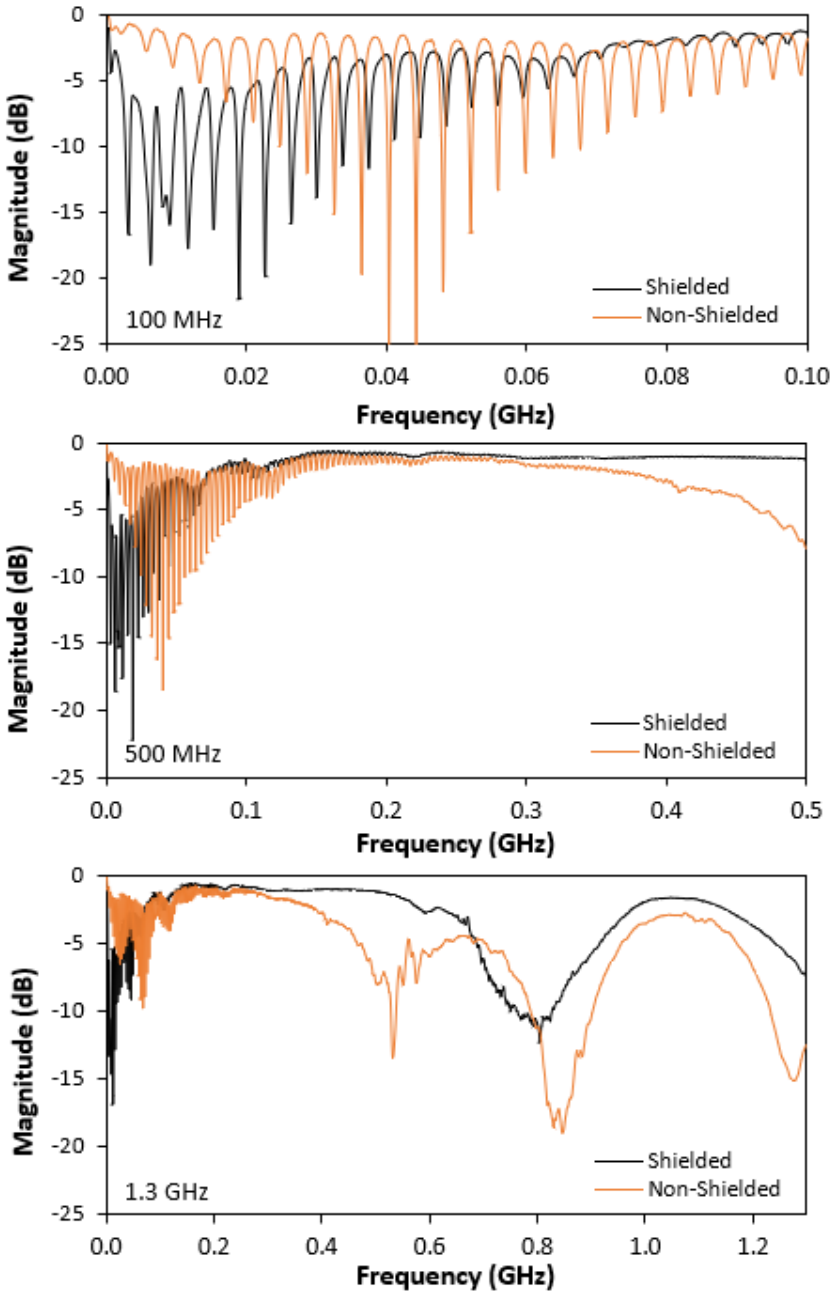


Figure 9-1. Frequency domain plots for the shielded (black) and non-shielded (orange) cables without a motor attached and no water.

First, the effect of the motor attached to the open end of the cables will be discussed. The magnitude of the reflected signal in the time domain is shown for the shielded and unshielded cables in Figure 9-2 and Figure 9-3, respectively. At each of the three measured frequencies, the solid line (—) represents the response acquired for the open-ended cable, the orange dotted line (---) represents the measured response of cable when connected to the motor, and the dotted line (– –) represents the absolute difference between the motor and no motor measurements. Both measurements were conducted in the absence of the water bath to independently evaluate changes in the cable response as a consequence of connecting the open end to a motor. For both shielded and unshielded cables, it was observed that the motor and no-motor cases were very similar across the evaluated frequency bandwidths. This observation was most strikingly apparent at the highest (1.3 GHz) frequency. At the lower frequency bandwidths (100 and 500 MHz),

differences on the order of 10 dB were observed between the motor and no-motor response curves from about 40 ft to the end of the cable. However, these differences between the motor and no-motor signals were small and lie within the range of the signal noise at these frequencies.

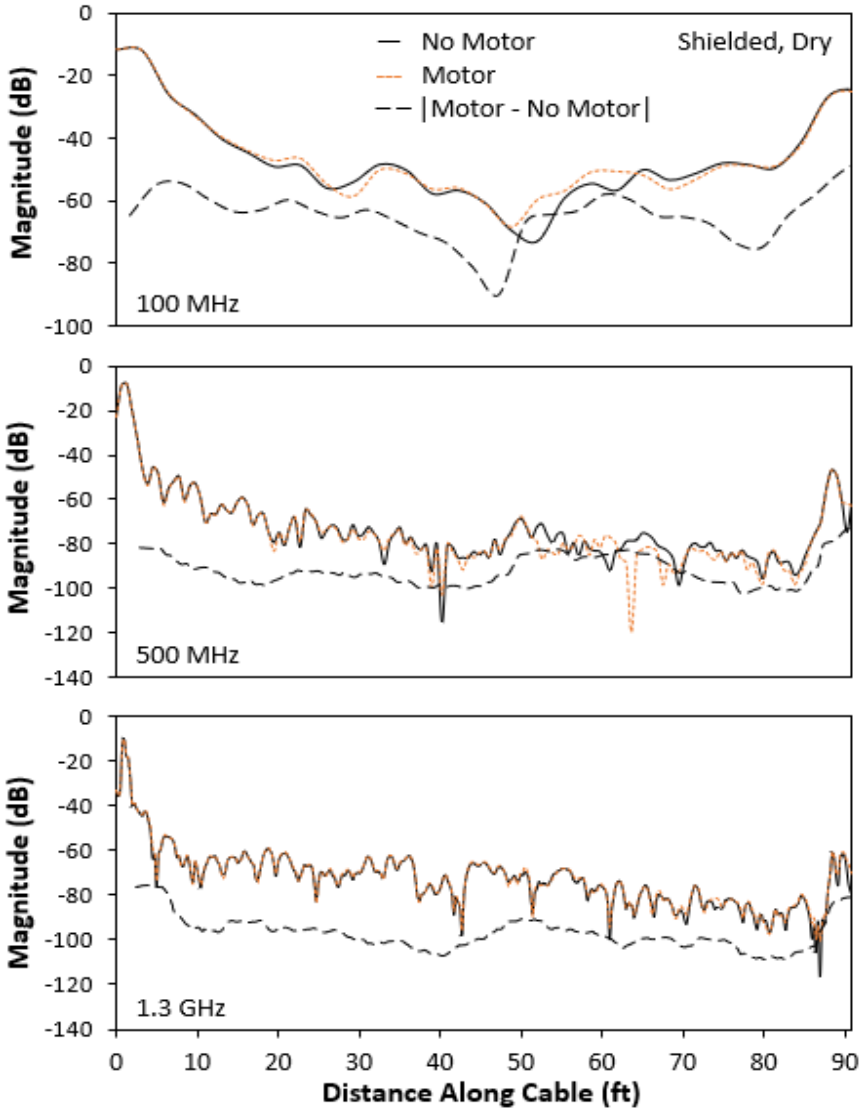


Figure 9-2. FDR time/distance domain response of the shielded cable with (---) and without (—) the motor attached at the selected bandwidths and no water present. The absolute difference with and without water is also indicated (– –).

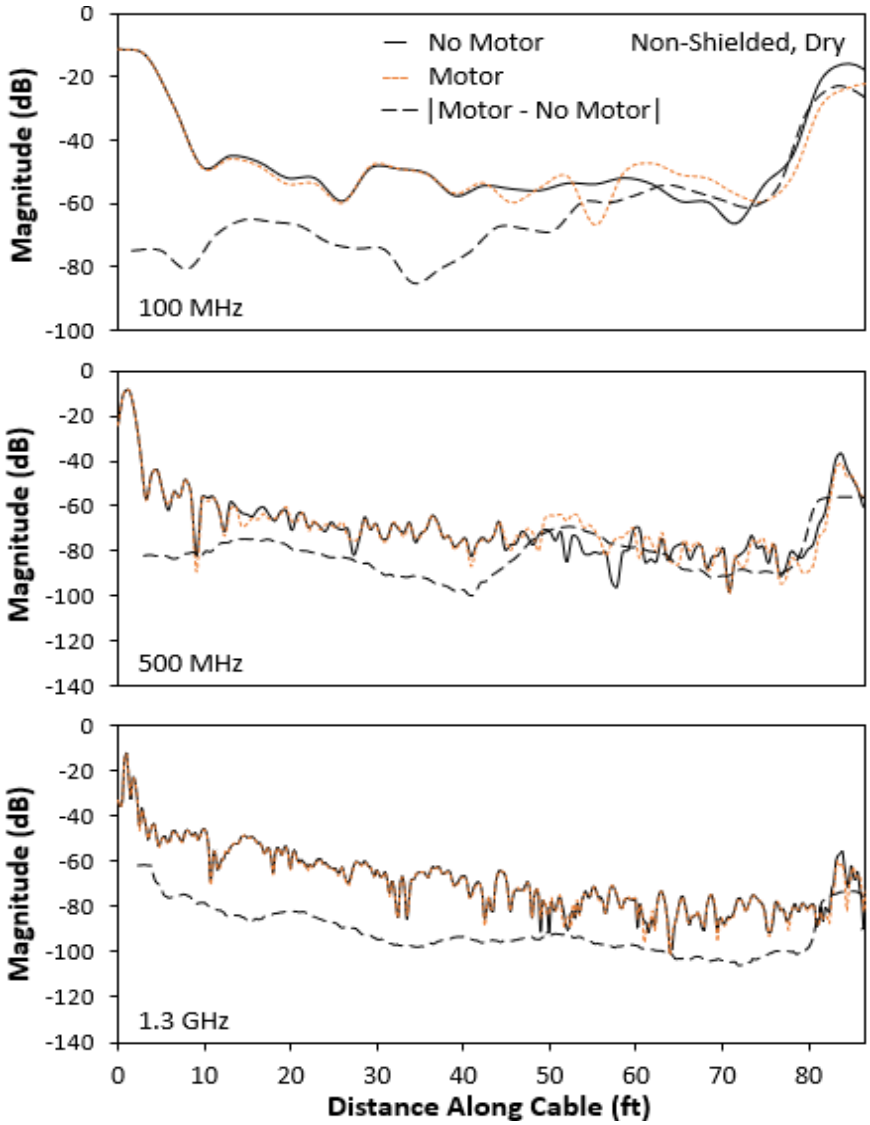


Figure 9-3. FDR time/distance domain response of the unshielded cable with (---) and without (—) the motor attached at the selected bandwidths and no water present. The absolute difference with and without water is also indicated (– –).

Next, the effect of partially submerging the cables in water on the time domain response will be discussed. In Figure 9-4 and Figure 9-5, the magnitude (in dB) of the signal response for the shielded and unshielded cable are shown. The response of the cable in the dry condition is shown by the solid line (—), whereas that of the partially submerged cable is shown by the dotted line (---). For all conditions, large peaks were observed in the range of 0 to 5 ft and 85 to 90 ft due to cable terminations. Of particular interest, and to be discussed in the next section, are the differences in cable response near the water bath location (see Table 8-3) between the dry and partially submerged cables.

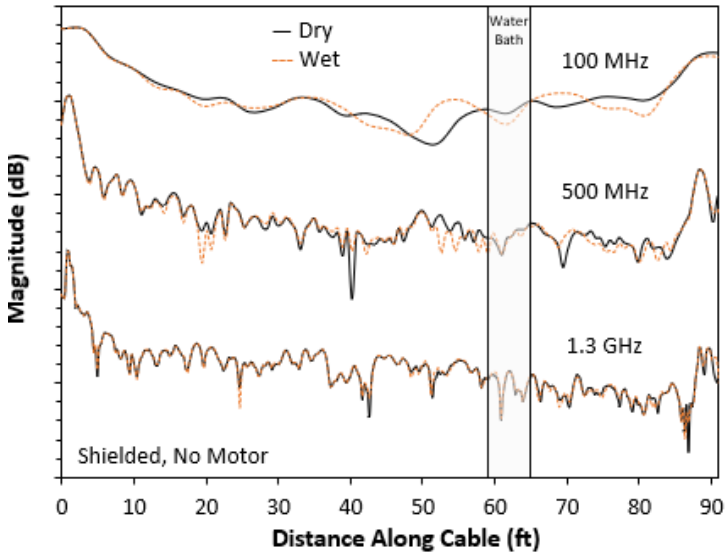


Figure 9-4. FDR time/distance domain response of the shielded cable with no motor attached at the dry (—) and wet (---) conditions for the selected bandwidths.

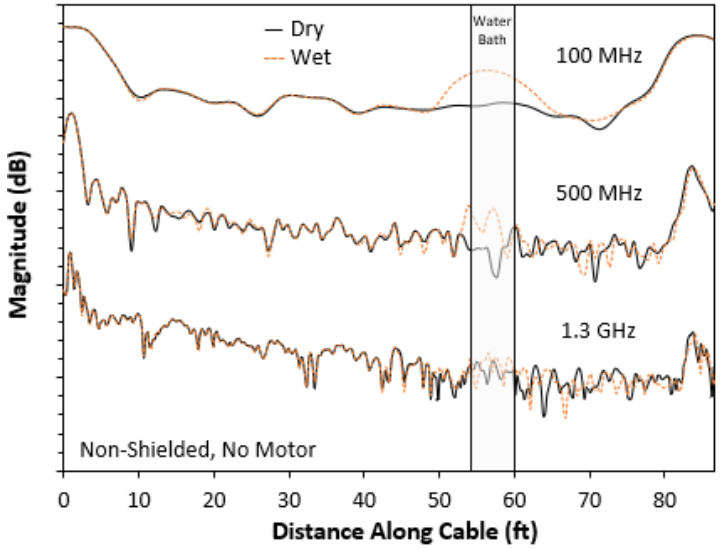


Figure 9-5. FDR time/distance domain response of the non-shielded cable with no motor attached at the dry (—) and wet (---) conditions for the selected bandwidths.

# 10. DISCUSSION

Taking a closer look at the absolute magnitude of the wet signal response of the shielded cable (Figure 10-1), two observations become apparent. First, as seen earlier in the dry case (Figure 9-2), connecting the cable to the motor does not significantly change the shape of the reflected signal at all three frequencies. Second, there is no clearly discernable peak in the response signal at the water bath location for all measurement conditions of the shielded cable. Likewise, for the non-shielded cable (also shown in Figure 10-1), the response of the cable when connected to the motor is very similar to that when it is disconnected. However, one or more peaks are introduced in the region of the water bath location for all three frequency bandwidths, with the largest water peak being observed for the 100 MHz frequency sweep. This large magnitude of the water peak at lower applied frequencies may be attributed to frequency-dependent

polarization mechanisms that are activated by the electromagnetic signal along the transmission line. Figure 10-2 shows the typical frequency ranges at which different polarization mechanisms may contribute to the electrical response of a dielectric material (such as, water, insulation or jacket (Ismail N.H. 2018). The maximum frequency range interrogated by the FDR test (300 kHz to 1.3 GHz) typically activates a dipolar (or orientational) polarization mechanism in dielectric materials (Dakin 2006). Based on molecular size, dipolar contribution is typically lost at frequencies greater than $10^9$-$10^{11}$ Hz which, in turn, results in a decrease in the response signal intensity. Consequently, the size of the water peak decreases with increasing applied frequency.

To evaluate moisture detection by FDR when the cable is partially exposed to water, time domain responses of the dry (dotted line) and wet (solid line) cable conditions are compared for the 100 MHz frequency sweep in Figure 10-3. For the shielded cable, neither the wet nor dry signals show a peak in the region of the water bath location, which indicates that exposure to moisture is not detected by this FDR test method when the shielded cable is partially submerged in water. Further studies on shielded cables using other test configurations are required to determine the feasibility of detecting water by FDR analysis on shielded cable. On the other hand, for the non-shielded cable, a large peak is observed in the wet signal at the location where it is submerged in water (the dry signal for the non-shielded cable does not have a peak in this region, see Figure 9-5). Consequently, the portion of the cable exposed to moisture is clearly detected by this method of FDR analysis for the non-shielded cable.

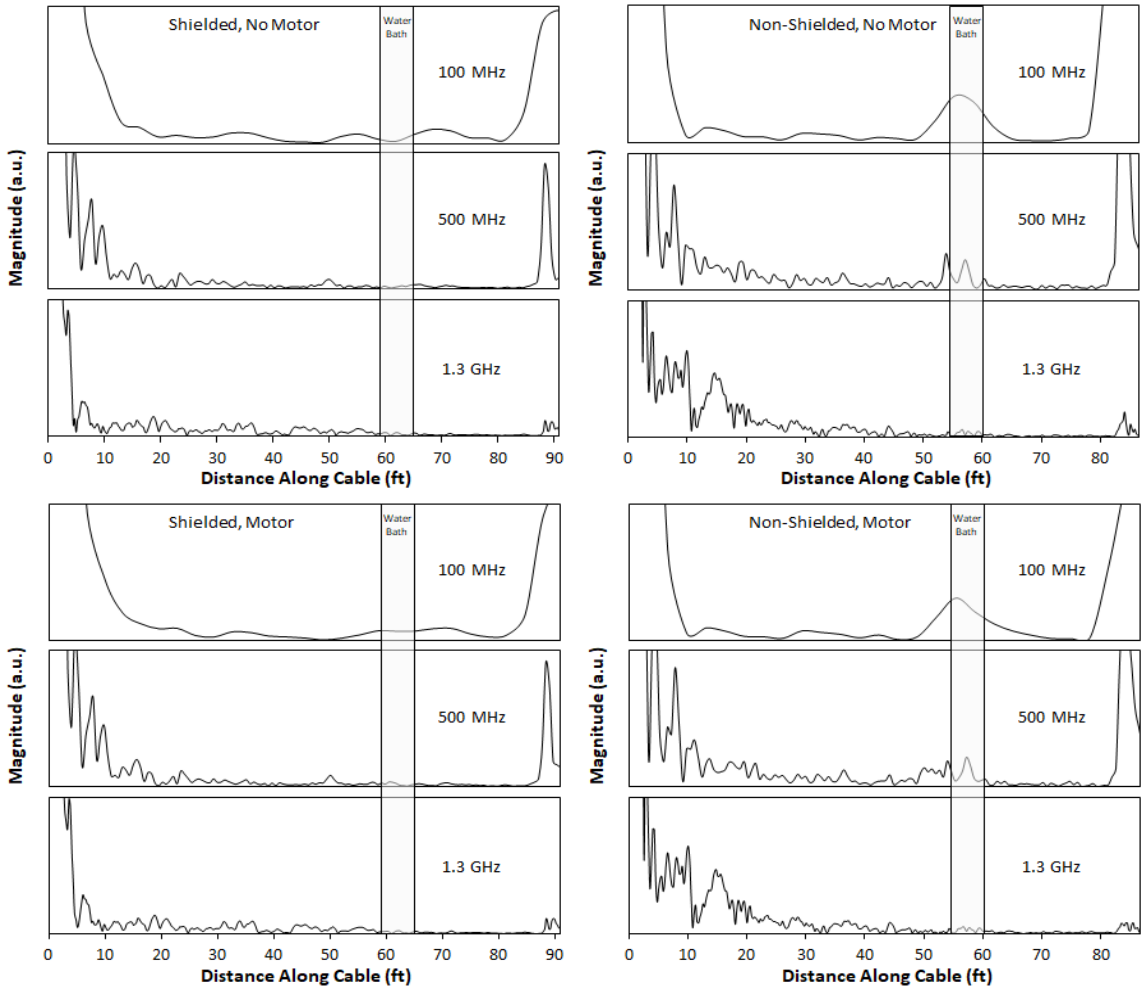


Figure 10-1. FDR time/distance domain magnitude response for the shielded and non-shielded cables with and without the motor attached. The location of the water bath is indicated in the figure. Magnitude variations at 0 to 5 ft and 85 to 90 ft are due to the terminations.

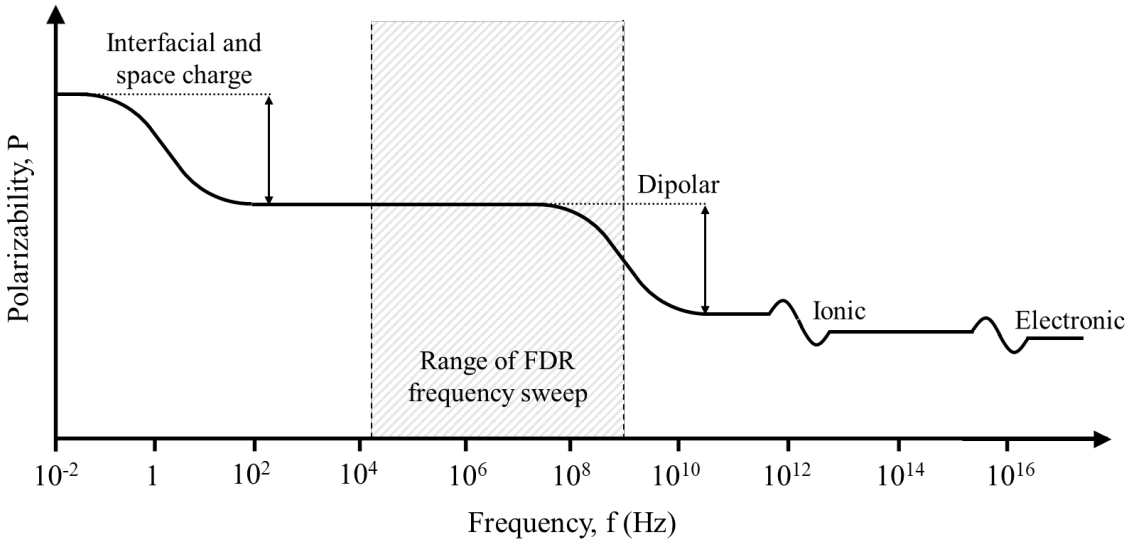


Figure 10-2. Frequency dependence of polarization mechanisms in a representative dielectric material.

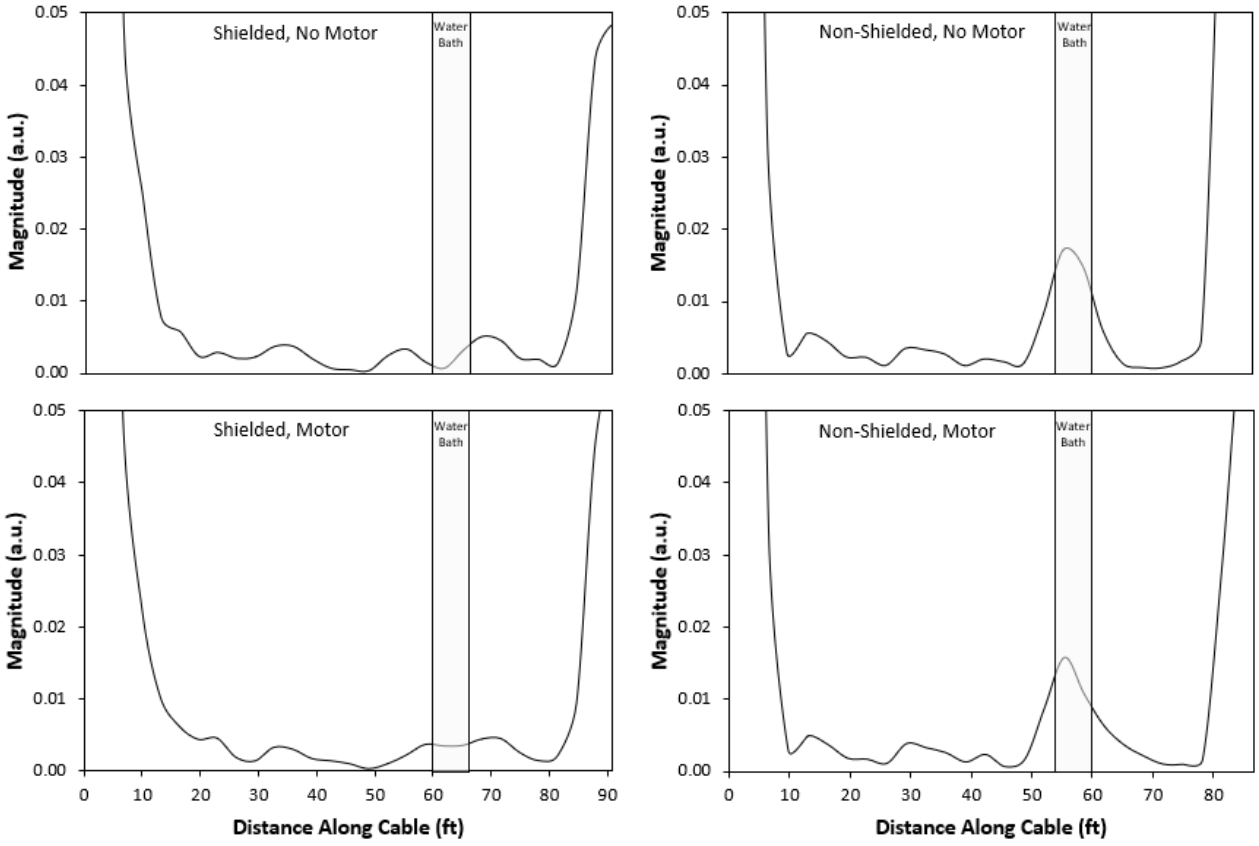


Figure 10-3. FDR time/distance domain magnitude response for the shielded and non-shielded cables with and without the motor attached at a bandwidth of 100 MHz. The location of the water bath is indicated in the figure.

# 11. OBSERVATIONS AND CONCLUSIONS

1. FDR spectra were equivalent with and without a motor being connected for both the shielded and non-shielded case.
2. FDR shows the presence of water for the non-shielded cable. Data taken at 0.1, 0.5, and 1.3 GHz bandwidth demonstrated remarkable peaks at the position corresponding to the water bath location along the cable. The peaks were significantly clearer with the 0.1 and 0.5GHz FDRs than with the 1.3GHz FDR.
3. FDRs did not show any indication of the presence or absence of water for shielded cable. As with the unshielded cable, data was taken at 0.1,0.5, and 1.3 GHz. No clear peaks were observed at the time corresponding to the cable immersion in the water bath location.
4. Water detection for the non-shielded cable by FDR analysis is frequency dependent with the largest signal response being observed at lower (100 MHz) frequencies. At the highest measurement frequency (1.3 GHz), the peaks were small and appear similar to noise. The absolute magnitude difference between the dry and wet signals in this region was < 10 dB. Whereas, for the measurement made at 100 MHz a large water peak was observed in the wet signal. The absolute magnitude difference was around 20 dB between wet and dry signals in the water bath region.
5. The ARENA test bed supported quick evaluation of cables by FDR analysis for several different configurations in a controlled environment.

# 12. REFERENCES


Agilent. 2012. *Time Domain Analysis Using a Network Analyzer.* Agilent Technologies, Santa Clara, California

Apogeeweb_Semiconductor_Electronic. 2016. "Twisted-Pair Impedance Calculator." accessed 09/16/2021. https://www.apogeeweb.net/tools/twisted-pair-impedance-calculator.html.

Chung, Y. C., N. N. Amarnath, and C. M. Furse. 2009. "Capacitance and Inductance Sensor Circuits for Detecting the Lengths of Open- and Short-Circuited Wires." *IEEE TRANSACTIONS ON INSTRUMENTATION AND MEASUREMENT* 58 (8):2495-2502. doi: 10.1109/Tim.2009.2014617.

Copper_Mountain. 2020. "Copper Mountain Compact VNA-TR1300/1." https://online.fliphtml5.com/pbaab/daxa/#p=1

Dakin, T.W. 2006. "Conduction and polarization mechanisms and trends in dielectric." *IEEE Electrical Insulation Magazine* 22:11-28. doi: 10.1109/MEI.2006.1705854.

Dubickas V., Edin H. 2004. "Couplers for on-line Time Domain Reflectometry diagnostics of power cables." Conference on Electrical Insulation and Dielectric Phenomena.

EE_Web. 2015. "Cable Impedance Calculator Twisted Pair." accessed 09/11/21. https://www.eeweb.com/tools/twisted-pair/.

Fifield, L S, M P Westman, A Zwoster, and B Schwenzer. 2015. *Assessment of Cable Aging Equipment, Status of Acquired Materials, and Experimental Matrix at the Pacific Northwest National Laboratory.* Pacific Northwest National Laboratory, Richland, Washington

Furse, C., Y. Chung, C. Lo, and P. Pendayala. 2006. "A critical comparison of reflectometry methods for location of wiring faults." *Smart Structures and Systems* 2 (1):25-46.

Furse, C., Y. Chung, D. Rakesh, M. Nelsen, G. Mabey, and R. Woodward. 2003. " Frequency Domain Reflectometry for On Board Testing of Aging Aircraft Wiring." *IEEE Trans. Electromagnetic Compatibility* 45 (2):306-315.

Furse, C., You Chung Chung, R. Dangol, M. Nielsen, G. Mabey, and R. Woodward. 2003. "Frequency-domain Reflectometry for On-board Testing of Aging Aircraft Wiring." *IEEE Transactions on Electromagnetic Compatibility* 45 (2):306-315. doi: 10.1109/TEMC.2003.811305.

Furse, C., P. Smith, M. Safavi, and C. Lo. 2005. "Feasibility of spread spectrum sensors for location of arcs on live wires." *EEE Sensors* 5 (6): 1445-1450.

Giaquinto N., Scarpetta M., Spadavecchia M. 2019. "Algorithms for Locating and chracterizing Cable Faults via Stepped-Frequency Waveform Reflectometry
" *IEEE Transactions on Instrumentation and Measurement* doi: doi={10.1109/TIM.2020.2974110}}.

Glass, S W, L S Fifield, G Dib, J R Tedeschi, A M Jones, and T S Hartman. 2015. *State of the Art Assessment of NDE Techniques for Aging Cable Management in Nuclear Power Plants FY2015.* Pacific Northwest National Laboratory, Richland, Washington

Glass, S W, L S Fifield, and T S Hartman. 2016. *Evaluation of Localized Cable Test Methods for Nuclear Power Plant Cable Aging Management Programs.* Pacific Northwest National Laboratory, Richland, Washington

Glass, S W, A M Jones, L S Fifield, and T S Hartman. 2016a. *Bulk Electrical Cable Non Destructive Examination Methods for Nuclear Power Plant Cable Aging Management Programs.* Pacific Northwest National Laboratory, Richland, Washington

Glass, S W, A M Jones, L S Fifield, and T S Hartman. 2016b. *Distributed Electrical Cable Non-Destructive Examination Methods for Nuclear Power Plant Cable Aging Management Programs.* Pacific Northwest National Laboratory, Richland, WA

Glass, S W, A M Jones, L S Fifield, T S Hartman, and N Bowler. 2017. *Physics-Based Modeling of Cable Insulation Conditions for Frequency Domain Reflectometry (FDR).* PNNL-26493, Pacific Northwest National Laboratory, Richland, Washington

Glass S.W., Fifield L.S., Bowler N. 2020. *PNNL 155612 Cable Nondestructive Examination Online Monitoring for Nuclear Power Plants.* Pacific Northwest National Laboratory, Richland Washington

Glass, Samuel W., Anthony M. Jones, Leonard S. Fifield, Nicola Bowler, Aishwarya Sriraman, and Roberto Gagliani. 2018. *Dielectric Spectroscopy for Bulk Condition Assessment of Low Voltage Cable -- Interim Report.* PNNL-27982 United States 10.2172/1491578 PNNL English, ; Pacific Northwest National Lab. (PNNL), Richland, WA (United States),

IAEA. 2012. *Assessing and Managing Cable Ageing in Nuclear Power Plants.* International Atomic Energy Agency (IAEA), Vienna

IEC. 2002. *Broadband Services, Applications, and Networks: Enabling Technologies and Business Models.* International Electrotechnical Commission (IEC),

Ismail N.H., Jaafar M. 2018. "A review of thermoplastic elastomeric nanocomposites for high voltage insulation applications." *Polymer ENgineering adn Science* 58 (S1). doi: 10.1002/pen>24882.

IWCE. 1996. "Frequency domain reflectometry vs. time domain reflectometry." IWCE. https://urgentcomm.com/1996/08/01/frequency-domain-reflectometry-vs-time-domain-reflectometry-here-are-the-fundamentals-of-two-measurement-technologies-and-a-nuts-and-bolts-look-at-the-practical-implications-for-rf-antenna-systems/.

Mantey, A. 2012. *EPRI Report 1025263 Plant Engineering: Dewatering Effects on Medium-Voltage Ethylene Propylene Rubber Cable.* EPRI, Palo Alto Ca.

Megger. 2020. "TDR900 Hand-held Time Domain Reflectometer/Cable Length Meter." https://www.globaltestsupply.com/pdfs/cache/www.globaltestsupply.com/tdr900/datasheet/tdr900-datasheet.pdf

Minet, J., S. Lambot, G. Delaide, J.A. Huisman, H. Vereecken, and M. Vanclooster. 2010. "A Generalized Frequency Domain Reflectometry Modeling Technique for Soil Electrical Properties Determination." *Vadose Zone Journal* 9 (4):1063-1072. doi: 10.2136/vzj2010.0004.

Mohr and Associates. 2010. *Application Note: TDR vs. FDR: Distance-to-Fault.* Mohr and Associates, Richland, Washington

Murty, K L, ed. 2013. *Materials Ageing and Degradation in Light Water Reactors: Mechanisms and Management*. Cambridge, United Kingdom: Woodhead Publishing.

Naik, S, C.M. Furse, and B.F. Boroujeny. 2006. "Multicarrier Reflectometry." *IEEE Sensors Journal* 6 (3): 812-818.

NRC. 2021. "Status of Subsequent License Renewal Applications." NRC, accessed 09/16/2021. https://www.nrc.gov/reactors/operating/licensing/renewal/subsequent-license-renewal.html

Simmons, K L, P Ramuhalli, D L Brenchley, and J B Coble. 2012. *Light Water Reactor Sustainability (LWRS) Program – Non-Destructive Evaluation (NDE) R&D Roadmap for Determining Remaining Useful Life of Aging Cables in Nuclear Power Plants.* Pacific Northwest National Laboratory, Richland, Washington

Smith, P. . 2003. *Spread Spectrum Time Domain Reflectometry (Ph.D. dissertation).* Utah State University,

Smith, P., C. Furse, and P. Kuhn. 2008. "Intermittent Fault Location on Live Electrical Wiring Systems." *SAE International*.

Tomain G., Brown K. 2004. "Medium Voltage Cable Wet Aging Concepts." EPRI, accessed 09/16/21. https://www.nrc.gov/docs/ML0418/ML041820194.pdf.

Tsai, P., Y. Chung, C. Lo, and C. Furse. 2005. "PMixed Signal Reflectometer Hardware Implementation for Wire Fault Location." *IEEE Sensors Journal* 5 (6):1479-1482.